NASA/TM—2000-210599

AIAA–2001–0164

5118 23
1N/07   16p

Performance Optimization of a Rotor Alone Nacelle for Acoustic Fan Testing

C.C. Cunningham, W.K. Thompson, and C.E. Hughes
Glenn Research Center, Cleveland, Ohio

December 2000

Since its founding, NASA has been dedicated to the advancement of aeronautics and space science. The NASA Scientific and Technical Information (STI) Program Office plays a key part in helping NASA maintain this important role.

The NASA STI Program Office is operated by Langley Research Center, the Lead Center for NASA's scientific and technical information. The NASA STI Program Office provides access to the NASA STI Database, the largest collection of aeronautical and space science STI in the world. The Program Office is also NASA's institutional mechanism for disseminating the results of its research and development activities. These results are published by NASA in the NASA STI Report Series, which includes the following report types:

- TECHNICAL PUBLICATION. Reports of completed research or a major significant phase of research that present the results of NASA programs and include extensive data or theoretical analysis. Includes compilations of significant scientific and technical data and information deemed to be of continuing reference value. NASA's counterpart of peer-reviewed formal professional papers but has less stringent limitations on manuscript length and extent of graphic presentations.

- TECHNICAL MEMORANDUM. Scientific and technical findings that are preliminary or of specialized interest, e.g., quick release reports, working papers, and bibliographies that contain minimal annotation. Does not contain extensive analysis.

- CONTRACTOR REPORT. Scientific and technical findings by NASA-sponsored contractors and grantees.

- CONFERENCE PUBLICATION. Collected papers from scientific and technical conferences, symposia, seminars, or other meetings sponsored or cosponsored by NASA.

- SPECIAL PUBLICATION. Scientific, technical, or historical information from NASA programs, projects, and missions, often concerned with subjects having substantial public interest.

- TECHNICAL TRANSLATION. English-language translations of foreign scientific and technical material pertinent to NASA's mission.

Specialized services that complement the STI Program Office's diverse offerings include creating custom thesauri, building customized data bases, organizing and publishing research results . . . even providing videos.

For more information about the NASA STI Program Office, see the following:

- Access the NASA STI Program Home Page at *http://www.sti.nasa.gov*

- E-mail your question via the Internet to help@sti.nasa.gov

- Fax your question to the NASA Access Help Desk at 301–621–0134

- Telephone the NASA Access Help Desk at 301–621–0390

- Write to:
  NASA Access Help Desk
  NASA Center for AeroSpace Information
  7121 Standard Drive
  Hanover, MD 21076

Performance Optimization of a Rotor Alone Nacelle for Acoustic Fan Testing

C.C. Cunningham, W.K. Thompson, and C.E. Hughes
Glenn Research Center, Cleveland, Ohio

National Aeronautics and
Space Administration

Glenn Research Center

December 2000

Acknowledgments

PERFORMANCE OPTIMIZATION OF A ROTOR ALONE NACELLE FOR ACOUSTIC FAN TESTING

C.C. Cunningham, W.K. Thompson, and C.E. Hughes
National Aeronautics and Space Administration
Glenn Research Center
Cleveland, Ohio 44135

Abstract

This paper describes the techniques, equipment, and results from the optimization of a two-axis traverse actuation system used to maintain concentricity between a sting-mounted fan and a wall-mounted nacelle in the 9'x15' (9 Foot by 15 Foot Test Section) Low Speed Wind Tunnel (LSWT) at the NASA Glenn Research Center (GRC). The Rotor Alone Nacelle (RAN) system, developed at GRC by the Engineering Design and Analysis Division (EDAD) and the Acoustics Branch, used nacelle-mounted lasers and an automated control system to maintain concentricity as thermal and thrust operating loads displace the fan relative to the nacelle. This effort was critical to ensuring rig/facility safety and experimental consistency of the acoustic data from a statorless, externally supported nacelle configuration. Although the tip clearances were originally predicted to be about 0.020" at maximum rotor (fan) operating speed, proximity probe measurements showed that the nominal clearance was less than 0.004". As a result, the system was optimized through control-loop modifications, active laser cooling, data filtering and averaging, and the development of strict operational procedures. The resultant concentricity error of RAN was reduced to ± 0.0031" in the Y-direction (horizontal) and +0.0035" / -0.0013" in the Z-direction (vertical), as determined by error analysis and experimental results. Based on the success of this project, the RAN system will be transitioned to other wind tunnel research programs at NASA GRC.

Introduction

One of the components of NASA's recently completed Advanced Subsonic Technology (AST) program was aircraft engine noise reduction. Previous wind tunnel testing under the Noise Element of the AST program identified several engine noise reduction concepts that contributed significantly to the successful achievement of the program's aggressive milestones. However, further investigation of the noise generating mechanisms in turbofan engines was needed if further noise reduction were to be achieved. The knowledge gained would lend itself to developing novel technologies targeted at specific noise areas in certain engine classes. As a result, an experimental program called the Source Diagnostic Test (SDT) was initiated for investigating these noise-generating mechanisms in the area of fan broadband noise. The investigation was carried out in the acoustically-treated NASA Glenn 9'x15' LSWT using 1/5 scale model hardware of a current generation high bypass turbofan aircraft engine.

The RAN project, an integral part of the SDT program, called for the development of an 'acoustically clean' flowpath within the nacelle to isolate the fan noise (i.e. one with no guide vanes, stators, or internal mounting struts that would contribute to the system acoustic signature). The only means of achieving such a design was to decouple the nacelle from the model centerbody. This required the nacelle to be mounted externally, independent of the fan and sting-mounted turbine drive system.

Engineers from EDAD and the Acoustics Branch at NASA GRC worked cooperatively to design and fabricate an externally supported nacelle and control system that would ensure concentricity of the fan and associated turbine drive system hardware with the nacelle during acoustic testing in the 9'x15' LSWT Shook et. al (Ref. 2) describes the design and integration process in greater detail. The nacelle would be

supported by two struts that attached to a 2-axis traverse table positioned outside the test section flow behind the tunnel walls (Figs. 1 & 2).

A nominal fan tip clearance of 0.020" was selected at the design point of 12,657 rpm (100% corrected fan speed) to reduce the risk of a fan incursion into the rubstrip. The design requirements stipulated that the nacelle's support structure be designed to minimize its acoustic signature to avoid contaminating the fan noise data. The wind tunnel would be operated at Mach 0.10, which simulated aircraft takeoff conditions, and the nacelle would be fixed at zero angle of attack. Table 1 outlines the pertinent test and model hardware parameters.

Parameter	Value
No. of Fan Blades	22
Fan Diameter (in.)	22
Fan Design Speed (rpm)	12,657
Max Corrected Fan Speed (100.7%)	12,746
Fan Design Pressure Ratio	1.47
Fan Thrust, approx. (lb$_f$)	1800
Test Section Freestream Mach No.	0.1

Table 1. Test and Performance Parameters

Concentricity of the fan within the nacelle was to be maintained as close as possible during testing to ensure a circumferentially uniform tip clearance and, therefore, uniform aerodynamic fan loading. In addition, if the radial concentricity offset exceeded 0.005" (indicating that the system was not operating properly), all motion of the RAN system would be halted. An earlier research study of fan model displacement, with the traditional stator-supported nacelle mounting method, found that the rotor face would pitch downward as much as -0.080" (Z-direction), yaw to one side 0.040" (Y-direction), and translate forward 0.125" (X-direction), due to thermal, aerodynamic and thrust loads. The thermal load was attributed mainly to the 450 psi, 600°F air that was plumbed through the sting to power the drive turbine. Nearby, the oil for the shaft bearings was cooled to 250°F. Additional thermal loads arose from fan exit flow (180°F) and external convection from Mach 0.1 airflow. Taken together, this combination of sources and sinks generated large thermal gradients that resulted in non-repeatable rig deformations.

The control system had to be rigid enough to prevent strut/nacelle excitation during tunnel operation and be accurate enough to control motion within 0.001". To ensure maximum stiffness, both the actuation table and nacelle struts were made of low
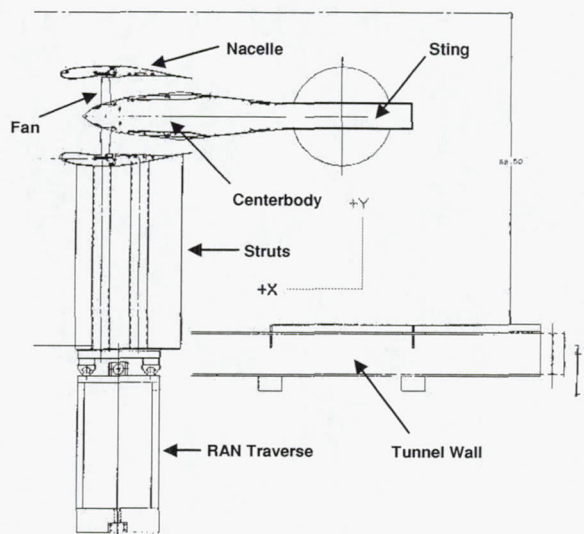
TOP VIEW

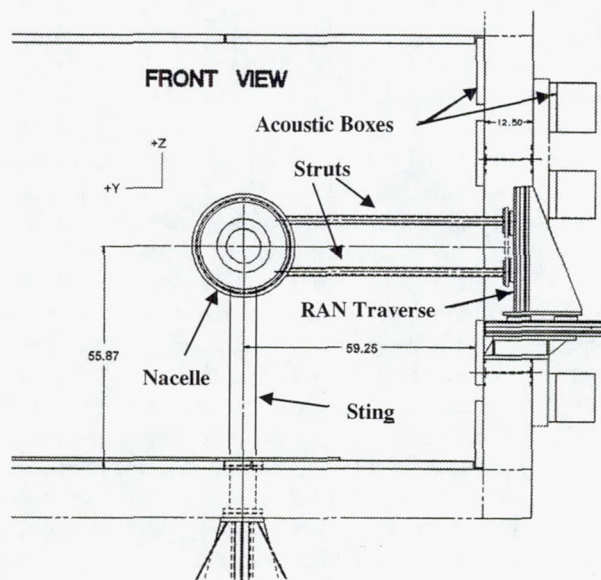Fig. 1. Top View of RAN System in 9'x15' LSWT

Fig. 2. Front View of RAN System in 9'x15' LSWT

carbon steel. Two servomotors (Kollmorgen Industrial Drives, model B-102-A-23) moved the table through two 100:1 gearboxes. Four nacelle-mounted laser displacement sensors measured the concentricity error, and a PC-based control system commanded the servomotors to move accordingly (Fig. 3). In addition to numerous software and hardware travel limits to maximize system safety, a ¾" highly ablative rub strip was incorporated into the nacelle to minimize any chance of damage to the fan blades during an incursion.

Position feedback came from the four laser displacement sensors (Micro Laser Sensor model LM10) located at 90-degree intervals around the center body. For RAN, two lasers actively were to provide positional data on the rotational plane (Y & Z), while the remaining two were to act as backups. Due to space constraints, the lasers could not be mounted with the beam directed radially; consequently, both the source and scatter signals were deflected 90° via polished aluminum plates. Bench tests confirmed the validity of this approach. The targets, which were 1" diameter flats machined on the centerbody, were located approximately 6.3" from their respective mirror. The laser configuration is shown in Fig. 4. The analog signals from the sensors were fed into a VersaLogic VL-1296 multi-purpose I/O card, as were the discrete signals for each laser sensor alarm, motor thermostats, axis faults and axis motion indicators. Discrete outputs from this card enabled motion and placed the servodrives in manual or automatic mode.

Due to the complexity of the RAN system and the safety issues involved, a comprehensive checkout of RAN was required prior to 9'x15' LSWT installation. The RAN traverse table was floor-mounted and qualified with the same hardware that would be used in the LSWT (Fig. 5). The target centerbody (w/ machined flats) was mounted to a controllable 2-axis traverse system (Probe Actuator Control System, or PACS) that provided motion to within 0.001", allowing the RAN system response to be compared against known inputs. Checks included manual and automatic operability, sampling rate, vibrational response, and failure modes. Since the main design goal of the RAN system was to prevent a fan rub into the casing, the checkout was conducted with fail-safe operation in mind. Three independent limit controls ensured that contact between the rotor tips and the metal casing beneath the rub strip would not be possible.

The RAN system was installed in the LSWT with exacting specifications to ensure that it was co-planar with the drive rig. A final checkout in the test section revealed no deviations from the previous checkout. One issue that could not be addressed during checkout was cooling of the laser units. Based on manufacturer specifications, the unit temperature could not exceed 120°F; beyond this, the measurement drift would become nonlinear and lead to unacceptable position errors. The maximum fan exit temperature, and hence, potential casing temperature, was predicted to be around 170°F. An insulation shield was incorporated between the laser and the casing; however, concern was raised that the insulator would not prevent

thermal soak during long test runs. Therefore, the laser mounts were modified to accommodate active cooling.

The lasers were raised about 1/8" off the casing, and nitrogen at ambient temperature was injected between the shield and the bottom of the unit. A sheet metal housing enclosed each laser and allowed the cooling gas to engulf the unit prior to discharge into the tunnel. Thermocouples with a ±1.0°F relative uncertainty were attached to the side of each laser unit (the location where enclosure temperatures were anticipated to be the highest) opposite from the nitrogen cooling tubes. Cooling pressure, laser temperature, nacelle excitation, and RAN position were monitored from an auxiliary control room.
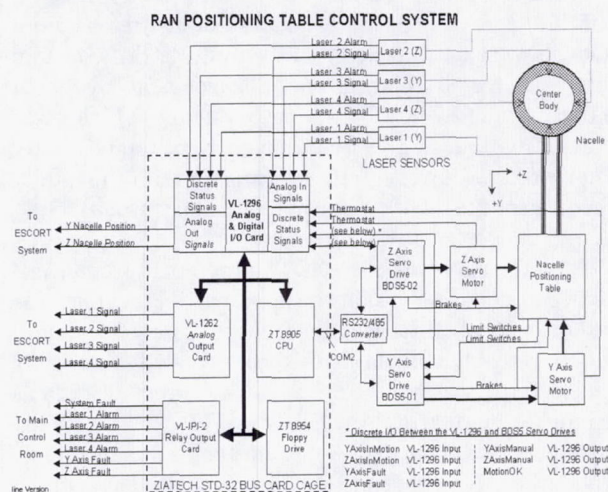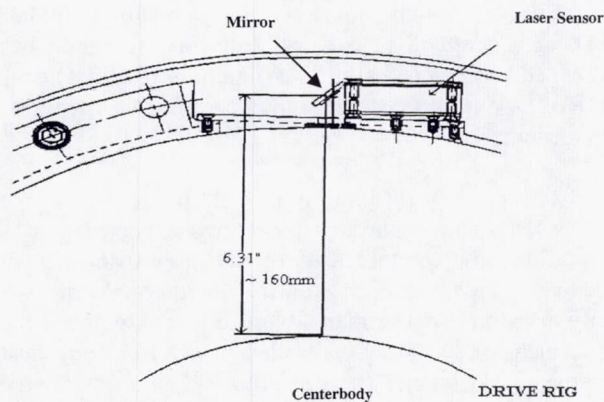

Fig. 3. RAN Hardware Schematic

Fig. 4. Side View of Displacement Sensor

Initial Results

During a check out test of the RAN system without a fan in the LSWT, the aerodynamic effects on the system were measured. As expected, the symmetry and stiffness of the struts prevented any measurable displacements. The first test with an operating fan was focused on identifying nacelle vibration and performing basic RAN control. Although the corrected fan speed was limited to 60%, the fan did not rub, and the nacelle excitation never exceeded the noise floor. A post-run impact test confirmed that the RAN system was highly damped. Fig. 6 shows a typical test configuration.

The first test of RAN at 100% corrected fan speed (w/ 0.004" deadband) resulted in a 0.020" rub, suggesting a total rig/nacelle non-concentricity of about 0.040". A review of the displacement and temperature data showed that the laser measurements drifted more than anticipated, biasing the displacement by about 0.015". The laser cooling system, which was previously untested, would have to be significantly improved. However, these findings did not fully account for the 0.040" error in radial concentricity.

As part of the SDT program, a standard configuration where stators supported the nacelle was installed to obtain baseline acoustic data. Proximity probe data obtained during this test revealed that the fan tip clearance was not 0.020" at 100% corrected speed as originally predicted. As shown in Fig. 7, the nominal clearance was only a few thousands of an inch. Therefore, the concentricity error would have to be dramatically reduced to prevent contact. Since the RAN rub strips were highly abradable and very thick, there were no concerns for the mechanical safety of the rig. However, the resultant fan offset could have a direct impact on acoustics by causing a non-uniform gap at the fan tips and, thus, asymmetric loading. In the case of a deep rub, the outer wall contour would be reshaped with step features. Numerous modifications to RAN would be necessary to accommodate the tight tip clearances.

Optimization Approach

The major hurdle to improving accuracy was controlling the thermal drift of the laser displacement readings. Test results showed that the thermal drift was only marginally better than advertised, mostly due to the placement of the laser controllers away from any heat source. Laser temperatures had reached an unanticipated 130°F, creating up to 0.017" of thermal drift. To control this, a three-pronged approach was developed: 1) cooling was improved to reduce ΔT, 2) the remaining drift was calculated using the backup lasers and incorporated into control loop, and 3) startup and centering procedures were developed to offset drift. First, the cooling was
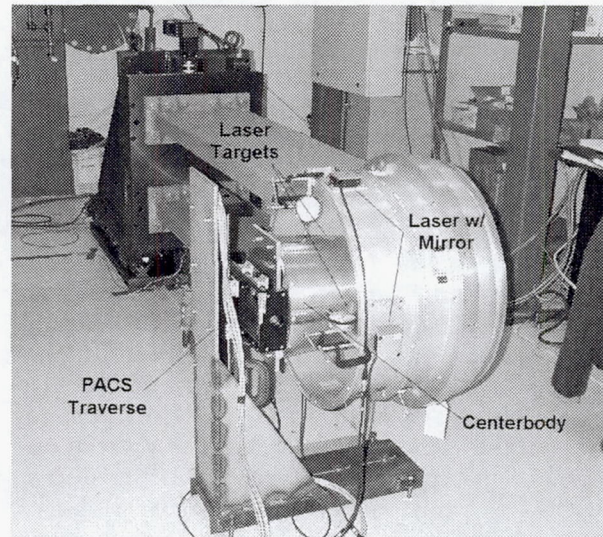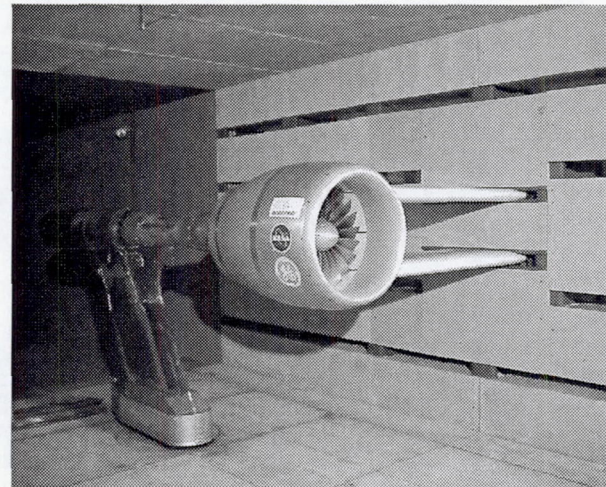

Fig. 5. Checkout of RAN w/PACS Traverse

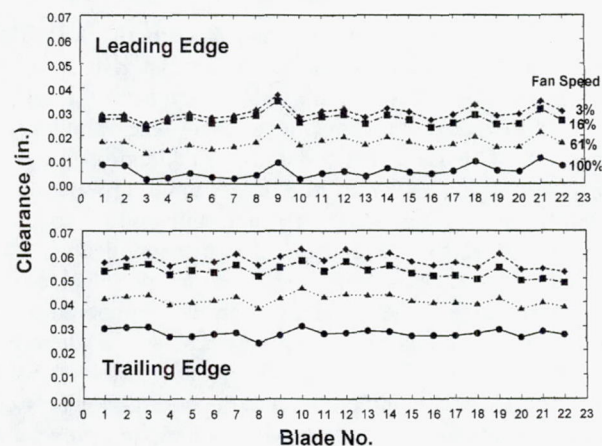Fig. 6. RAN hardware in the 9'x15' LSWT

Fig. 7. Tip Clearance Results

improved by maximizing the nitrogen flowrate to facility capacity through larger cooling lines and fluted tubes at each laser unit. A heat exchanger was created from copper tubing running through an ice-water bath, and the lines from the bath to the lasers were insulated. This reduced the nitrogen temperature at the laser head by 30°F. The cooling tube position was closely scrutinized to ensure uniform cooling around the laser units.

Second, the amount of error introduced by the thermal drift effect was calculated. With the exception of the unit mounted near the attachment of the strut (Laser 3, as shown in Fig. 8), each laser unit had nearly identical temperature response during testing. Because of its proximity to the nacelle/external strut attachment point, laser 3 was exposed to a larger heat source. The maximum cooling flow rate supplied to laser 3 was insufficient to reduce the enclosure temperature to the level of the other three lasers. However, since the other units stayed consistent, the net effect was similar to a common mode source of error on a differential measurement. As the nacelle temperature rose, the output readings from each laser rose by roughly the same amount. A correction factor was obtained by computing the arithmetic average of two lasers mounted directly opposite from one another on the nacelle. This average represents the common mode component due to thermal drift. By subtracting this common mode component from the control laser readings of all four lasers before computing the required table motion, the effect of the thermal drift was greatly reduced.

Third, a startup and centering procedure was developed. The lasers were powered one hour prior to test, self-heating them to their maximum steady-state temperature (~90°F). With the table in manual mode, the rotor was centered within the nacelle using dial indicators. The laser controllers were then zeroed, and the cooling system was opened. Once the lasers cooled to about 60°F, the test could begin. This technique forced the lasers to a negative offset position at startup. As the test progressed, the thermal offset would shift from negative to positive – the result was a reduction in absolute drift. Since tip clearances were quite large and data was not taken at low speeds, the negative drift had no impact on the RAN hardware or data. By the time acoustic testing was initiated, the laser enclosure temperature had stabilized to pretest levels.

Beyond drift, another challenge arose from the electrical noise found in the 9'x15' LSWT facility. Installing 8-pole, 5 Hz Butterworth instrumentation filters on the laser displacement signal lines improved system performance somewhat, but additional software filtering was still needed. The solution was to change

the laser position sampling rate and sample time. Averaging several hundred samples per scan provided excellent noise immunity. The effective sampling rate became 0.5 Hz; however, the motion of the centerbody due to thermal and thrust loads was predictably slow, as long as fan ramp rate was kept at 25 rpm/sec or less. Thus, the compromise in control system response time was not an issue. Conversely, the accuracy gain was significant enough to allow for control system operation with a 0.0015" deadband - better than the design requirements. It was noted that the slow response of the control system would virtually ensure a fan rub during an emergency shutdown while at high fan speeds and thrust loads. This was deemed acceptable, as twelve inspected rub strips were available and emergency shutdowns were rare.
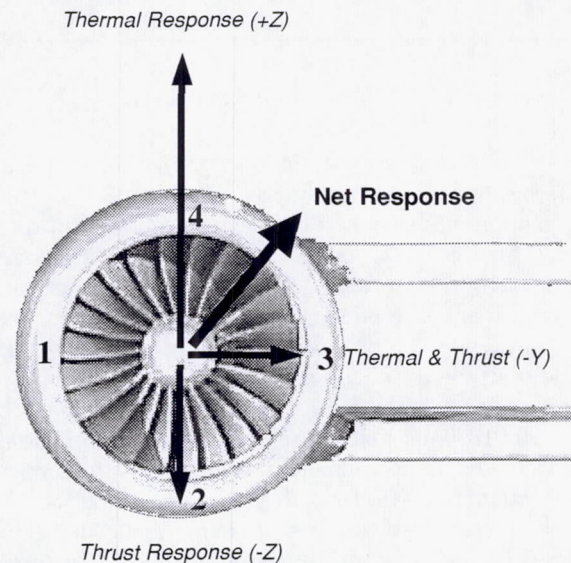

Thermal Response (+Z)

Net Response

4

1

3 *Thermal & Thrust (-Y)*

2

Thrust Response (-Z)

Fig. 8. Characteristic Displacement Vectors
(w/ Lasers Numbered)

Final Results

Implementing the techniques described above improved performance dramatically. Table 2 shows the modifications and the approximate contribution to centering accuracy for a typical run at 100.7% corrected fan speed. Most of the values were gathered from test data; however, many of the improvements were implemented coincidentally, so exact values are subject to some degree of interpretation. Table 3 provides a summary of fan rub events after the system was fully optimized. Only two of the 19 runs following optimization resulted in contact as a result of the non-concentricity error; three other rubs were caused by hardware or facility issues.

Error Source	Modification	Improvement
Thermal Drift	Drift Correction	0.008"
Excessive Heat / Drift	Improved Cooling	0.005"
Feedback Precision	Software Filtering	0.002"
Thermal Drift	Offset Procedure	0.002"
Facility Noise	Hardware Filtering	0.001"
Total Reduction		**0.018"**

Table 2. Optimization Summary

Rub Type	No. of tests	Cause
None	11 @ 100.7%	N/A
	3 @ <100.7%	
Slight glazing (<0.002")	2 @ 100.7%	Error band
Significant rub (>0.002")	1 @ 100.7%	Rub strip loose
	1 @ <100.7%	Emergency shutdown
	1 @ <100.7%	Laser fault

Table 3. Rub Results

With the system optimized, the displacement data becomes more meaningful. Prior to RAN, drive rig motion was assumed dependent primarily on rotor speed for slow ramp rates. The sample data from five runs to 100.7% corrected fan speed (Figs. 9 and 10) showed this not to be the case. It should be noted that the position data was recorded only at steady-state conditions and does not represent every move performed by the system. Displacement differences of over 0.010" and 0.030" in the Y and Z-directions, respectively, were common even on tests with identical configurations. In fact, displacement could not be directly correlated to overall ramp rate, idle time, ambient conditions, or rig modifications. Therefore, maintaining concentricity by utilizing historical displacement data in a passive control system would most likely be unsuccessful.

Despite the quantitative variations in displacement, the qualitative motion was quite consistent. Also, observations during emergency shutdowns showed the effects of thermal and thrust loads on displacement. As thrust quickly relieved, only the thermal component remained. The rig would jump ~0.050" in the +Z-direction then slowly return to its initial position as the system cooled. Fig. 8 illustrates the relative contributions of thermal and thrust loads to rig displacement, along with location of the four lasers. To obtain a clear understanding of the system's final concentricity error, the drift data was thoroughly examined. Figs. 11 shows the uncorrected drift as a function laser temperature for five separate runs. Drift did not correlate well with RPM, but was clearly a

linear function of the change of laser temperature, ΔT (0.0037"/deg). Since drift was linear and the correction was a based on averaging, the residual drift could be calculated from the differences in ΔT of opposing lasers. The residual drift was found by multiplying half of the laser temperature difference by the individual drift slope for that run (Fig. 12). In the Z-direction, the temperature rise always favored Laser 2, presumably due to local equilibrium conditions. Consequently, the offset always biased in the same direction (-Z). The slopes of the residual drift curves were very consistent, with a mean slope of 0.00020"/deg and a standard deviation of only 0.000017"/deg.

The availability of error data from testing and manufacturer's specifications allowed for a thorough dissection of concentricity. Kline and McClintock (Ref. 1) present a technique for determining the propagation of errors in a derived result for single-sample experiments. If ω_i represents the uncertainty of a variable, and there are n independent variables or simultaneous measurements [e.g., $R=R(X_1,X_2,X_3,...,X_n)$], the uncertainty in the result is given by:

$$\omega_R = \pm\left[\left(\frac{\partial R}{\partial X_1}\omega_1\right)^2 + \left(\frac{\partial R}{\partial X_2}\omega_2\right)^2 + \cdots + \left(\frac{\partial R}{\partial X_n}\omega_n\right)^2\right]^{1/2} \quad (1)$$

for a 95% confidence interval (CI). However, the concentricity error included known offsets - the deadband was a precisely controlled offset, and the residual laser drift was measured with consistency. Since the absolute drift calculation was dependent on other error sources included in the total uncertainty, it was treated as a known bias (+0.0011"±0.0003") in the Z-direction, and the concentricity was fully penalized by +0.0011". The value for source uncertainty were determined only at max speed where tip clearances were smallest; therefore, the concentricity error ($E_{95\%CI}$) can be expressed as the sum of the known offsets (C_i) and the uncertainty (ω_R) as follows:

$$E_{95\%CI} = \left(\sum C_i\right) \pm \omega_R \quad (2)$$

If the deadband is treated as part of the total uncertainty, Eq. 2 yields +0.0029"/-0.0007" in the Z-direction. This result provides a 95% CI *at any instance in time*. However, the system requires a perceived non-concentricity of 0.0015" prior to correction. To obtain an estimate of concentricity error with 95% CI *immediately prior to correction,* the deadband must be treated as a fixed bias that fully penalizes the
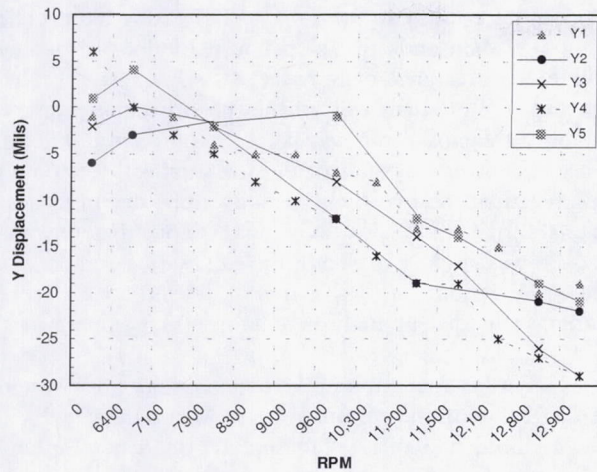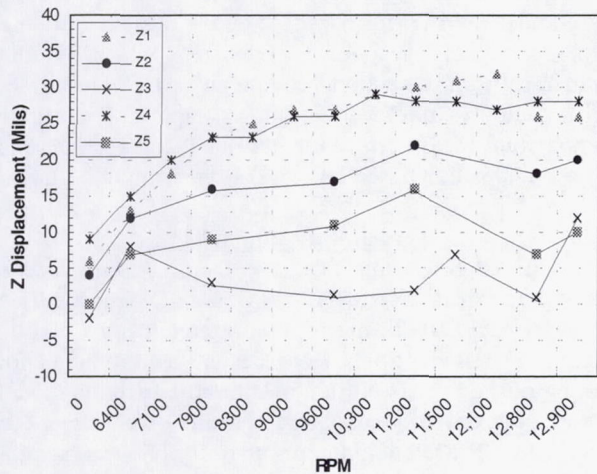
Fig. 9. Y-axis Absolute Position vs. RPM

Fig. 11. Laser Drift vs. Sensor Temp

Fig. 10. Z-axis Absolute Position vs. RPM

Fig. 12. Residual Drift after Correction

concentricity. If the uncertainties and offsets are defined by U and C, respectively, the concentricity error was calculated as follows:

$$E_{95\%CI} = C_{drift\_offset} \pm C_{deadband} \qquad (3)$$
$$\pm \left[\left(U_{drift\_variation} \right)^2 + \left(U_{centering} \right)^2 + \cdots + \left(U_{response\_lag} \right)^2 \right]^{1/2}$$

This increases the Z-direction error to +0.0036"/-0.0014", which better reflects the accuracy of the system for our purposes.

The concentricity error in the Y-direction was determined in the same manner, with the exception of the laser drift values. Since the readings from Laser 3 were ignored (due to higher temperature relative to the
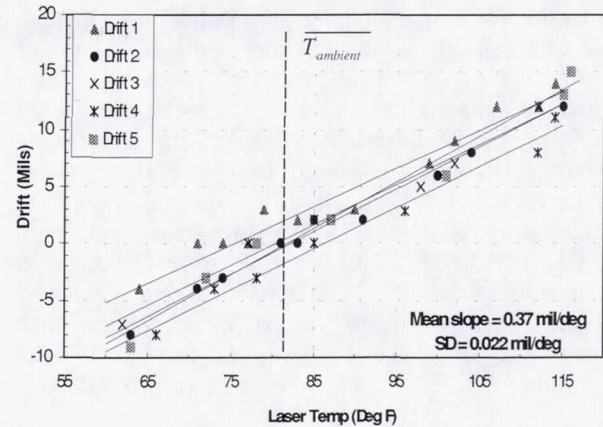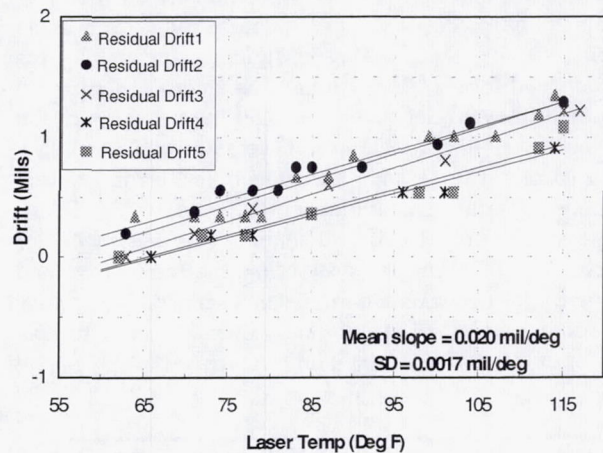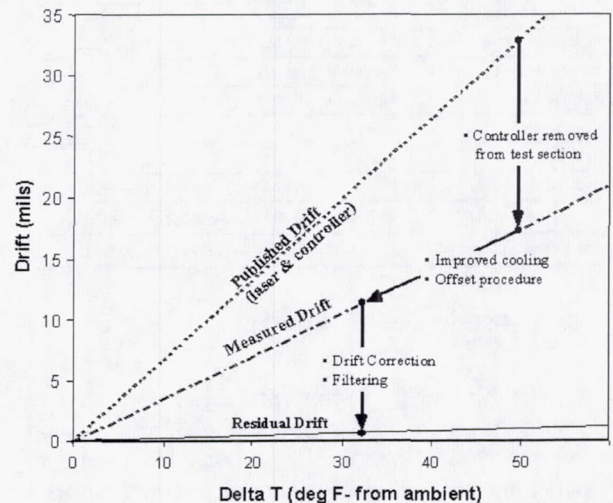

Fig. 13. Drift Reduction Chart

other three lasers), averaging was not possible. Instead, the offset from the Z-axis was applied to Laser 1 reading. This was considered an acceptable approach, since the temperature rise (ΔT) of Laser 1 always fell between that of Lasers 2 and 4. If the temperature change of Laser 1 was exactly equal to average change of Laser 2 and 4, then the drift error was minimized ($\pm 0.003"$). If $\Delta T_1 = \Delta T_2$, the drift error would be $-0.0011" \pm 0.0003"$. Conversely, if $\Delta T_1 = \Delta T_4$, the drift error would be $+0.0011" \pm 0.0003"$. Since ΔT_1 seemed to vary randomly between ΔT_2 and ΔT_4, a drift uncertainty of $\pm 0.0014"$ was applied in the Y-direction. This led to a total error in Y of $\pm 0.0032"$.

A summary of the data and results from the concentricity analysis can be found in Table 4. Fig. 13 shows the reduction in drift slope, along with the effects of cooling and offset. A few comments on the error sources are necessary. The quantization error was an artifact of the analog-to-digital conversion, as calculated for a 12-bit system. The values for corrected laser drift were dependent only on the accuracy of the temperature measurements. If we assume a worst case scenario, where the thermocouple error caused opposing laser temperatures to diverge by 2.0°F, the effect on residual drift calculation was only 10%, or about 0.0001". As for system lag, the ramp rates (and hence rig displacements) never exceeded 25 rpm/s, leading to minimal system lag. Even so, an ample lag error of 0.0005" was assumed for each axis.

Error Source	Type	Z Error (in.)	Y Error (in.)
Centering	Bias	± 0.0005	± 0.0005
Table position	Precision	negligible	negligible
Table repeatability	Precision	± 0.0002	± 0.00020
Signal resolution	Precision	± 0.0002	± 0.00020
Signal linearity error	Precision	negligible	negligible
Quantization error	Precision	± 0.00025	± 0.00025
Electrical noise	Random	± 0.0005	± 0.0005
Target finish	Precision	± 0.00025	± 0.00025
Response lag	Random	± 0.0005	± 0.0005
Deadband	Bias	± 0.0015	± 0.0015
Corrected laser drift	Bias	+0.0011 ± 0.0003	± 0.0014
Total Error (Instant.)	95% CI	**0.0029 / -0.0007**	**± 0.0023**
Total Error (@deadband)	95% CI	**0.0036 / -0.0014**	**± 0.0032**

Table 4. Concentricity Errors at 100.7% Speed

The findings of concentricity analysis were supported by test results. Tip clearance probes could not be incorporated into the low-density foam strip, so the only indication of non-concentricity came from tests in which rubs occurred. Prior to optimization, rub strip contact consistently occurred on the top half of the rub strip, indicating a slight bias in the +Z-direction and a random uncertainty in the Y-axis. Offsetting the nacelle by a few thousands of an inch usually led to glazing where the clearance was reduced. One test revealed glazing on more than 180° of the rub strip; interestingly, the only area not to rub was between 4:00 and 8:00 (-Z), where the error was statistically the smallest. Even after optimization, the two 'concentricity' rubs occurred near the 10:00 and 2:00 positions, again indicating that the nacelle was slightly biased in the +Z, but was random in the Y-direction. Although not quantitative, these findings support our analysis of concentricity error.

Further reduction in the concentricity error would be difficult with the current system. When the deadband was reduced to 0.001", 'hunting' (defined here as any unwarranted motion) was present, although infrequent. Even so, this was deemed undesirable since test requirements dictated a totally stable platform during acoustic data acquisition at steady-state conditions. Stabilization at smaller deadbands would require additional filtering, further slowing the system response time, or high response hardware, which would dramatically raise cost and complexity. However, laser drift could be further reduced by supplying accurate temperature measurements to the feedback system, and adjusting position based on correlations from this study.

Concluding Remarks

Based on results from the Rotor Alone Nacelle project part of the NASA Glenn Source Diagnostic Test in the 9'x15' LSWT, the following conclusions can be drawn: 1) All control system design requirements for testing of the bypass portion of a turbofan engine model with an externally-supported nacelle were met or exceeded; 2) Maintaining concentricity between a rotor and an externally-supported nacelle during testing in a wind tunnel environment is feasible, even with extremely tight tip clearances; 3) Although characteristics have been established, the displacement of the drive rig in NASA Glenn Research Center's 9'x15' LSWT is not consistent enough to exclude an active control system for maintaining a uniform fan tip clearance at all model operating conditions.

The use of thermally-cooled opposing laser units allowed for a massive reduction in thermal drift, along with backup control in the event of a unit failure. This technique resulted in better concentricity than that of a single displacement feedback system. The key to high accuracy was the consistent temperature rise across opposing lasers.

The optimization steps described in this paper maximized the performance possible with the existing hardware. Reductions to the residual drift could only be achieved by either utilizing lasers that are more

thermally tolerant or incorporating temperature compensation into the system. Other error reductions would add unwarranted cost for minimal gains.

Future tests will likely include analog recording of displacement, temperature, and drift data – this would allow better understanding of thermal and thrust loads, especially when recorded from an emergency shutdown where the thermal displacement can be isolated. Addition of the third axis for axial control (X-direction) is planned for another project and is not expected to present any new challenges.

References
1.   Kline, S.J. and McClintock, F.A., "Describing Uncertainties in Single-Sample Experiments", *Mechanical Engineering* 75:3-8, 1953.

2.   Shook, T.A., Hughes, C.E., Thompson, W.K., Tavernelli, P.F., Cunningham, C.C., and Shah, A.R., "Design and Integration of a Rotor Alone Nacelle for Acoustic Fan Testing", AIAA Paper 2001-1058, Jan. 2001.

REPORT DOCUMENTATION PAGE

Public reporting burden for this collection of information is estimated to average 1 hour per response, including the time for reviewing instructions, searching existing data sources, gathering and maintaining the data needed, and completing and reviewing the collection of information. Send comments regarding this burden estimate or any other aspect of this collection of information, including suggestions for reducing this burden, to Washington Headquarters Services, Directorate for Information Operations and Reports, 1215 Jefferson Davis Highway, Suite 1204, Arlington, VA 22202-4302, and to the Office of Management and Budget, Paperwork Reduction Project (0704-0188), Washington, DC 20503.

1. AGENCY USE ONLY *(Leave blank)*	2. REPORT DATE December 2000	3. REPORT TYPE AND DATES COVERED Technical Memorandum

4. TITLE AND SUBTITLE

Performance Optimization of a Rotor Alone Nacelle for Acoustic Fan Testing

5. FUNDING NUMBERS

WU–940–30–09–21

6. AUTHOR(S)

C.C. Cunningham, W.K. Thompson, and C.E. Hughes

7. PERFORMING ORGANIZATION NAME(S) AND ADDRESS(ES)

National Aeronautics and Space Administration
John H. Glenn Research Center at Lewis Field
Cleveland, Ohio 44135–3191

8. PERFORMING ORGANIZATION REPORT NUMBER

E–12557

9. SPONSORING/MONITORING AGENCY NAME(S) AND ADDRESS(ES)

National Aeronautics and Space Administration
Washington, DC 20546–0001

10. SPONSORING/MONITORING AGENCY REPORT NUMBER

NASA TM—2000-210599
AIAA–2001–0164

11. SUPPLEMENTARY NOTES

Prepared for the 39th Aerospace Sciences Meeting and Exhibit sponsored by the American Institute of Aeronautics and Astronautics, Reno, Nevada, January 8–11, 2001. Responsible person, C.C. Cunningham, organization code 7725, 216–433–5516.

12a. DISTRIBUTION/AVAILABILITY STATEMENT

Unclassified - Unlimited
Subject Categories: 07, 09, 33, and 37   Distribution: Nonstandard

Available electronically at http://gltrs.grc.nasa.gov/GLTRS

This publication is available from the NASA Center for AeroSpace Information, 301–621–0390.

12b. DISTRIBUTION CODE

13. ABSTRACT *(Maximum 200 words)*

This paper describes the techniques, equipment, and results from the optimization of a two-axis traverse actuation system used to maintain concentricity between a sting-mounted fan and a wall-mounted nacelle in the 9×15 (9 Foot by 15 Foot Test Section) Low Speed Wind Tunnel (LSWT) at the NASA Glenn Research Center (GRC). The Rotor Alone Nacelle (RAN) system, developed at GRC by the Engineering Design and Analysis Division (EDAD) and the Acoustics Branch, used nacelle-mounted lasers and an automated control system to maintain concentricity as thermal and thrust operating loads displace the fan relative to the nacelle. This effort was critical to ensuring rig/facility safety and experimental consistency of the acoustic data from a statorless, externally supported nacelle configuration. Although the tip clearances were originally predicted to be about 0.020 in. at maximum rotor (fan) operating speed, proximity probe measurements showed that the nominal clearance was less than 0.004 in. As a result, the system was optimized through control-loop modifications, active laser cooling, data filtering and averaging, and the development of strict operational procedures. The resultant concentricity error of RAN was reduced to ±0.0031 in. in the Y-direction (horizontal) and +0.0035 in./–0.0013 in. in the Z-direction (vertical), as determined by error analysis and experimental results. Based on the success of this project, the RAN system will be transitioned to other wind tunnel research programs at NASA GRC.

14. SUBJECT TERMS

Rotor blades; Turbomachinery; Fan; Wind tunnel models; Active control; Nacelles; Acoustics

15. NUMBER OF PAGES

15

16. PRICE CODE

A03

17. SECURITY CLASSIFICATION OF REPORT Unclassified	18. SECURITY CLASSIFICATION OF THIS PAGE Unclassified	19. SECURITY CLASSIFICATION OF ABSTRACT Unclassified	20. LIMITATION OF ABSTRACT